Research Square

Preprints are preliminary reports that have not undergone peer review.
They should not be considered conclusive, used to inform clinical practice,
or referenced by the media as validated information.

Stability and Bifurcation Dynamics of a Discrete-Time Predator-Prey Model with Proportional Harvesting

M. A. Rouf Emon

abdurrouf@eub.edu.bd

European University of Bangladesh

Sarna Sarker

Daffodil International University

Jahidul Islam

Daffodil International University

M. Humayun Kabir

Jahangirnagar University

Research Article

Keywords:

Posted Date: November 12th, 2026

DOI: https://doi.org/10.21203/rs.3.rs-11672715/v1

License: This work is licensed under a Creative Commons Attribution 4.0 International License.
Read Full License

Additional Declarations: No competing interests reported.

Stability and Bifurcation Dynamics of a Discrete-Time Predator-Prey Model with Proportional Harvesting

M. A. Rouf Emon[1], Sarna Sarker[2], Jahidul Islam[3], M. Humayun Kabir[4]

[1]Department of Mathematics, European University of Bangladesh
[2, 3]Daffodil International University
[1, 4]Mathematical and Computational Biology (MCB) Group, Department of Mathematics, Jahangirnagar University, Dhaka-1342, Bangladesh
[4]Center for Mathematical Modeling and Applications (CMMA), Meiji University, 164-8525 Tokyo, Japan
Corresponding author. E-mail: abdurrouf@eub.edu.bd

Abstract

The paper deals with a comprehensive analysis of a discrete-time model of prey-predator with proportional harvesting in the prey population. We show the positivity and boundedness of solutions which is relevant for the biological viability. Rigorous proofs for the existence and uniqueness of the three equilibria—extinction, prey-only, and coexistence—are shown. A detailed sensitivity analysis for the parameters is carried out and local stability conditions are derived with the help of the Jury criterion. The analytical calculation of the first Lyapunov coefficient is carried out to show the super-critical character of the Neimark-Sacker bifurcation. Theoretical results are validated by numerical simulations, such as time-series, phase portraits, bifurcation diagrams and stability maps. We show that the proportional harvesting is a double-edged sword, it both reduces population densities, and yet it can suppress chaotic oscillations at moderate harvesting intensity. Our findings can be used to offer quantitative recommendations for sustainable harvesting in ecological management.

Keywords: Discrete-time models, Stability, Neimark-Sacker bifurcation, Jury conditions, MSY.

AMS Subject classification(2020): 39A30, 39A28, 92D25, 92D40, 49N90.

1 Introduction

Many species, including the majority of fish stocks, annual plants and many insects, have non-overlapping generations, for which there can be no alternative to a discrete-time ecological model to understand population dynamics. [1]. Of these, the predator prey relations are one of the fundamental approaches to the study of density dependent growth and interspecific relations. Although mathematically tractable, continuous-time Lotka-Volterra models often don't account for the complicated oscillations that arise from over compensatory density dependence. Ricker-type discrete maps, characterized by the exponential growth term $N_t \exp(r(1 - N_t/K))$, are particularly notorious for generating period-doubling routes to chaos [2, 3] and Neimark-Sacker bifurcations when coupled with predator functional responses [4, 5].

These ecosystems face a change in their stability landscape when harvested intentionally (fisheries) or unintentionally (habitat loss). The harvesting method of constant yield and constant effort has been studied extensively in recent years in the literature. [6] and nonlinear harvesting [7]. However, in the discrete-time Ricker-predator context, proportional (or constant-effort) harvesting—in which the amount gathered grows linearly with population density—remains comparatively unexplored. Because proportional harvesting is an idealization of catch-per-unit-effort (CPUE) fisheries from a biological perspective, it is extremely pertinent to sustainable management.

We build on the classical density-dependent discrete predator-prey model of Beddington, Free & Lawton [9], which combines Ricker-type host growth with a Nicholson–Bailey escape response, as presented in standard texts (e.g., Murray [8]). The unharvested version of this model has been analyzed for global stability by Din [10]; here we extend the analysis to incorporate proportional harvesting, deriving new results on equilibrium existence, stability, sensitivity, and Neimark–Sacker bifurcation.

The main novelty of this work is threefold: (i) We rigorously derive the existence and uniqueness conditions for the interior equilibrium under proportional harvesting, revealing a critical threshold $aK(1+\ln(1-h)/r) > 1$ that governs predator invasion. **(ii)** We provide the analytical normal form for the

Neimark-Sacker bifurcation, explicitly computing the first Lyapunov coefficient following the standard normal-form machinery [20] and in the spirit of related analytical derivations for discrete-time predator-prey systems [17, 18, 19], and resolve the sign convention discrepancies using topological validation from phase portraits. **(iii)** We perform a comprehensive parameter sensitivity analysis (both analytical and graphical) to rank the influence of each ecological parameter on system stability, complementing existing stability and chaos-control studies of discrete-time predator-prey systems [16, 15, 31], and identifying the harvesting rate as the most influential control parameter. **(iv)** We derive a closed-form Maximum Sustainable Yield (MSY) at the prey-only equilibrium and show it is ecologically inconsistent with predator persistence, motivating a two-species-consistent MSY criterion at the coexistence equilibrium – a harvesting-invasion trade-off not addressed in related discrete-time bifurcation studies [11, 12, 13, 6, 14, 30].

2 Model Formulation

We consider the following discrete-time prey-predator mathematical model:

$$\begin{aligned} N_{t+1} &= (1-h)N_t \exp\left[r\left(1-\tfrac{N_t}{K}\right) - aP_t\right], \\ P_{t+1} &= N_t(1-\exp(-aP_t)), \end{aligned} \tag{1}$$

where N_t denotes the prey population density and P_t the predator population density at time t. The ecological parameters are defined as:

- $r > 0$: Intrinsic growth rate of prey.
- $K > 0$: Environmental carrying capacity.
- $a > 0$: Predator attack rate.
- $h \in (0, 1)$: Proportional harvesting rate.

Remark 2.1. *The predator equation $P_{t+1} = N_t(1-e^{-aP_t})$ follows the classical Nicholson–Bailey escape-response formulation [21, 22, 23], in which e^{-aP_t} is the (Poisson-derived) probability that a prey individual escapes attack. This places system (1) within the discrete-time host–parasitoid modelling tradition [24] rather than a Lotka–Volterra-type predator–prey framework. We retain the terms "prey" and "predator" throughout for readability and consistency with the harvesting-fishery literature [29], but the results apply directly to host–parasitoid systems (e.g. biological pest control) [26, 27, 25], where N_t and P_t represent host and parasitoid densities, respectively.*

3 Non-negativity and Boundedness of Solutions of the Model

3.1 Non-negativity of Solutions

To ensure ecological validity, we prove that trajectories initiated in the first quadrant remain non-negative.

Theorem 3.1. *Every trajectory of system (1) with initial conditions $N_0 \geq 0$ and $P_0 \geq 0$ remains in $\mathbb{R}^2_+$ for all $t > 0$.*

Proof. Given $0 < h < 1$, we have $1 - h > 0$. The exponential function is strictly positive for all real arguments. Hence, from the prey equation:

$$N_{t+1} = (1-h)N_t \exp\left[r\left(1-\frac{N_t}{K}\right) - aP_t\right] \geq 0,$$

since $N_t \geq 0$ and the exponential term is positive. For the predator equation, since $P_t \geq 0$, we have $0 < \exp(-aP_t) \leq 1$, which implies $1 - \exp(-aP_t) \geq 0$. Therefore,

$$P_{t+1} = N_t(1-\exp(-aP_t)) \geq 0.$$

Thus, the non-negative quadrant $\mathbb{R}^2_+$ is positively invariant. □

3.2 Boundedness of Solutions

Theorem 3.2. *All solutions of system (1) are uniformly bounded within a compact region* $\Omega = \{(N, P) \in \mathbb{R}^2_+ : 0 \le N \le C, 0 \le P \le C\}$ *for some* $C > 0$.

Proof. From the prey equation, since $\exp(-aP_t) \le 1$, we obtain

$$N_{t+1} \le (1-h)N_t \exp\left(r\left(1 - \frac{N_t}{K}\right)\right).$$

Define $f(N) = N\exp(r(1 - N/K))$. Differentiating with respect to N:

$$f'(N) = \exp\left(r\left(1 - \frac{N}{K}\right)\right)\left(1 - \frac{rN}{K}\right).$$

Setting $f'(N) = 0$ yields the critical point $N = K/r$. The maximum value is

$$f_{\max} = \frac{K}{r}e^{r-1}.$$

Thus,

$$N_{t+1} \le (1-h)\frac{K}{r}e^{r-1} =: M.$$

Let $C = \max\{N_0, P_0, M\}$. Then $N_t \le C$ for all $t \ge 0$. For the predator,

$$P_{t+1} = N_t(1 - \exp(-aP_t)) \le N_t \le C.$$

Hence, both populations are uniformly bounded. □

4 Equilibrium Analysis

A steady state (N^*, P^*) satisfies the equilibrium conditions:

$$N^* = (1-h)N^* \exp\left[r\left(1 - \frac{N^*}{K}\right) - aP^*\right], \quad P^* = N^*(1 - \exp(-aP^*)). \tag{2}$$

4.1 Extinction Equilibrium

If $N^* = 0$, then from the second equation of (2) we get $P^* = 0$. Hence, the trivial equilibrium always exists:

$$E_0 = (0, 0).$$

4.2 Predator-free Equilibrium

Assume $P^* = 0$ and $N^* > 0$. Substituting $P^* = 0$ into the first equation of (2) gives:

$$1 = (1-h)\exp\left[r\left(1 - \frac{N^*}{K}\right)\right].$$

Taking logarithms:

$$0 = \ln(1-h) + r\left(1 - \frac{N^*}{K}\right).$$

Solving for N^*:

$$\frac{rN^*}{K} = r + \ln(1-h),$$
$$N^* = K\left(1 + \frac{\ln(1-h)}{r}\right).$$

Thus, the prey-only equilibrium is

$$E_1 = \left(K\left(1 + \frac{\ln(1-h)}{r}\right), 0\right).$$

This equilibrium is biologically feasible (i.e., $N^* > 0$) if and only if

$$r > -\ln(1-h).$$

4.3 Coexistence Equilibrium

For the interior equilibrium $E_2 = (N^*, P^*)$, we assume $N^* > 0$ and $P^* > 0$. From the first equation of (2), dividing by N^* and taking logarithms yields the prey nullcline:

$$\frac{rN^*}{K} + aP^* = r + \ln(1-h). \tag{3}$$

From the second equation, since $P^* > 0$, we have

$$P^* = N^*(1 - e^{-aP^*}) \quad \Longrightarrow \quad N^* = \frac{P^*}{1 - e^{-aP^*}}.$$

Substituting this into (3) gives the transcendental equation for P^*:

$$\frac{K}{r}\left[r + \ln(1-h) - aP^*\right] = \frac{P^*}{1 - e^{-aP^*}}. \tag{4}$$

Theorem 4.1. *The interior equilibrium E_2 exists uniquely in $\mathbb{R}^2_+$ if and only if*

$$aK\left(1 + \frac{\ln(1-h)}{r}\right) > 1.$$

Proof. Define the continuous function

$$\Phi(P) = \frac{K}{r}\left[r + \ln(1-h) - aP\right] - \frac{P}{1 - e^{-aP}},$$

on the interval $P \in \left(0, \frac{r+\ln(1-h)}{a}\right)$. As $P \to 0^+$, using L'Hôpital's rule on the second term:

$$\lim_{P\to 0^+} \frac{P}{1 - e^{-aP}} = \frac{1}{a}.$$

Thus,

$$\begin{aligned}\lim_{P\to 0^+} \Phi(P) &= \frac{K}{r}\left[r + \ln(1-h)\right] - \frac{1}{a} \\ &= K\left(1 + \frac{\ln(1-h)}{r}\right) - \frac{1}{a}.\end{aligned}$$

This limit is positive if and only if $aK\left(1 + \frac{\ln(1-h)}{r}\right) > 1$. At the upper endpoint $P_{\max} = \frac{r+\ln(1-h)}{a}$, we have

$$\Phi(P_{\max}) = 0 - \frac{P_{\max}}{1 - e^{-aP_{\max}}} < 0.$$

Since Φ is continuous and strictly decreasing (as shown below), the Intermediate Value Theorem guarantees a unique root $P^* \in (0, P_{\max})$. To show monotonicity, compute the derivative:

$$\Phi'(P) = -\frac{aK}{r} - \frac{(1 - e^{-aP}) - aPe^{-aP}}{(1 - e^{-aP})^2}.$$

The numerator of the second fraction is $\psi(P) = 1 - e^{-aP} - aPe^{-aP}$. Note that $\psi(0) = 0$ and $\psi'(P) = a^2Pe^{-aP} > 0$ for $P > 0$. Hence $\psi(P) > 0$, so the second fraction is positive. Therefore, $\Phi'(P) < 0$, establishing uniqueness. Substituting P^* back into $N^* = P^*/(1-e^{-aP^*})$ gives a unique positive N^*. □

5 Local Stability and Sensitivity Analysis of the Steady States

The Jacobian matrix of system (1) at any point (N, P) is:

$$J(N,P) = \begin{pmatrix} (1-h)\exp\left[r\left(1-\frac{N}{K}\right) - aP\right]\left(1 - \frac{rN}{K}\right) & -(1-h)aN\exp\left[r\left(1-\frac{N}{K}\right) - aP\right] \\ 1 - \exp(-aP) & aN\exp(-aP) \end{pmatrix}.$$

5.1 Stability of $E_0(0, 0)$

At E_0, the Jacobian becomes:

$$J(E_0) = \begin{pmatrix} (1-h)e^r & 0 \\ 0 & 0 \end{pmatrix}.$$

The eigenvalues are $\lambda_1 = (1-h)e^r$ and $\lambda_2 = 0$. Hence, E_0 is locally asymptotically stable if $|\lambda_1| < 1$, i.e.,

$$(1-h)e^r < 1 \quad \Longleftrightarrow \quad r < -\ln(1-h).$$

If $r > -\ln(1-h)$, then $\lambda_1 > 1$, making E_0 unstable.

5.2 Stability of $E_1(\overline{N}, 0)$

At E_1, using the equilibrium condition $(1-h)\exp(r(1-\overline{N}/K)) = 1$, the Jacobian simplifies to:

$$J(E_1) = \begin{pmatrix} 1 - \frac{r\overline{N}}{K} & -a\overline{N} \\ 0 & a\overline{N} \end{pmatrix}.$$

The eigenvalues are

$$\lambda_1 = 1 - \frac{r\overline{N}}{K} = 1 - (r + \ln(1-h)), \quad \lambda_2 = a\overline{N} = aK\left(1 + \frac{\ln(1-h)}{r}\right).$$

Thus, E_1 is locally asymptotically stable if both $|\lambda_1| < 1$ and $|\lambda_2| < 1$. These conditions yield:

$$0 < r + \ln(1-h) < 2, \quad \text{and} \quad aK\left(1 + \frac{\ln(1-h)}{r}\right) < 1.$$

If $\lambda_2 > 1$, the predator can invade the prey-only state, rendering E_1 unstable.

5.3 Stability of $E_2(N^*, P^*)$

At E_2, the equilibrium condition $(1-h)\exp(r(1-N^*/K) - aP^*) = 1$ holds. The Jacobian is:

$$J(E_2) = \begin{pmatrix} 1 - \frac{rN^*}{K} & -aN^* \\ 1 - e^{-aP^*} & aN^*e^{-aP^*} \end{pmatrix}.$$

Let T and D denote the trace and determinant:

$$T = 1 - \frac{rN^*}{K} + aN^*e^{-aP^*}, \tag{5}$$

$$D = aN^*\left[1 - \frac{rN^*}{K}e^{-aP^*}\right]. \tag{6}$$

The characteristic equation is $\lambda^2 - T\lambda + D = 0$. According to the Jury stability criterion [2], E_2 is locally asymptotically stable if and only if:

$$1 + T + D > 0, \tag{7}$$

$$1 - T + D > 0, \tag{8}$$

$$1 - D > 0. \tag{9}$$

5.4 Parameter Sensitivity Analysis

To quantify the robustness of each equilibrium, we compute the sensitivity (first-order partial derivatives) of the dominant eigenvalues with respect to the parameters r, K, a, h.

5.4.1 Sensitivity of the Steady States at E_0

The only nontrivial eigenvalue is $\lambda_1 = (1-h)e^r$. Its derivatives are:

$$\begin{aligned}
\frac{\partial \lambda_1}{\partial r} &= (1-h)e^r = \lambda_1 > 0, \\
\frac{\partial \lambda_1}{\partial h} &= -e^r < 0, \\
\frac{\partial \lambda_1}{\partial K} &= 0, \\
\frac{\partial \lambda_1}{\partial a} &= 0.
\end{aligned}$$

Thus, an increase in r destabilizes E_0, while an increase in h stabilizes it. The parameters K and a have no effect on the local extinction dynamics.

5.4.2 Sensitivity of the Steady States at E_1

For the predator-invasion eigenvalue $\lambda_2 = aK(1 + \ln(1-h)/r)$, we compute:

$$\frac{\partial \lambda_2}{\partial h} = -\frac{aK}{r(1-h)} < 0, \tag{10}$$

$$\frac{\partial \lambda_2}{\partial r} = -\frac{aK \ln(1-h)}{r^2} > 0 \quad (\text{since } \ln(1-h) < 0), \tag{11}$$

$$\frac{\partial \lambda_2}{\partial a} = K\left(1 + \frac{\ln(1-h)}{r}\right) > 0, \tag{12}$$

$$\frac{\partial \lambda_2}{\partial K} = a\left(1 + \frac{\ln(1-h)}{r}\right) > 0. \tag{13}$$

For the prey-mode eigenvalue $\lambda_1 = 1 - (r + \ln(1-h))$, we have:

$$\frac{\partial \lambda_1}{\partial r} = -1 < 0, \quad \frac{\partial \lambda_1}{\partial h} = \frac{1}{1-h} > 0.$$

These results show that harvesting suppresses predator invasion ($\partial\lambda_2/\partial h < 0$), while high prey growth promotes it ($\partial\lambda_2/\partial r > 0$).

5.4.3 Sensitivity of the Steady States at E_2

The sensitivity of T and D with respect to h is obtained via implicit differentiation of the equilibrium equations (closed-form derivation given in Section 5.5). At the nominal parameter set $r = 2.4, K = 10, a = 0.35$, evaluated at the precise Neimark–Sacker threshold $h^* \approx 0.199193$ (see Appendix A), we obtain:

$$\left.\frac{dN^*}{dh}\right|_{h^*} \approx -1.6394, \quad \left.\frac{dP^*}{dh}\right|_{h^*} \approx -2.4437,$$

and consequently,

$$\left.\frac{dD}{dh}\right|_{h^*} \approx -0.6668 < 0.$$

This confirms the transversality condition for the Neimark-Sacker bifurcation. The normalized sensitivity indices at a stable regime ($h = 0.25$) are summarized in Table 1.

Table 1: Normalized sensitivity indices of T and D at E_2 for $r = 2.4$, $K = 10$, $h = 0.25$.

Parameter	**Sensitivity of T**	**Sensitivity of D**	**Stability Impact**
r	$+0.1245$	-0.0321	Increasing r reduces stability
a	-0.0873	-0.0154	Slightly stabilizes
h	-0.2418	-0.1092	Strongly stabilizes

5.5 Analytical Transversality Condition for the Neimark–Sacker Bifurcation

The numerical value $dD/dh|_{h^*} \approx -0.6666$ reported in Section 5.4.3 follows from a general closed-form expression, which we now derive. This confirms that the transversality condition holds not merely at an isolated parameter point, but throughout a well-defined region of parameter space.

Differentiating the equilibrium conditions (2) implicitly with respect to h, and writing $N_h := dN^*/dh$, $P_h := dP^*/dh$, the prey equilibrium condition gives

$$\frac{r}{K}N_h + aP_h = -\frac{1}{1-h}, \tag{14}$$

while the predator equilibrium condition gives

$$P_h = N_h \frac{1-e^{-aP^*}}{\Delta}, \qquad \Delta := 1 - aN^*e^{-aP^*}. \tag{15}$$

Substituting (15) into (14) and solving for N_h:

$$N_h = \frac{-1}{(1-h)\left[\dfrac{r}{K} + \dfrac{a(1-e^{-aP^*})}{\Delta}\right]}. \tag{16}$$

Recall from (6) that $D = aN^*\left(1 - \dfrac{rN^*}{K}e^{-aP^*}\right)$. Differentiating with respect to h and substituting (15) and (16) yields, after simplification,

$$\frac{dD}{dh} = aN_h\left[1 - \frac{2rN^*}{K}e^{-aP^*} + \frac{arN^{*2}}{K\Delta}e^{-aP^*}\left(1-e^{-aP^*}\right)\right]. \tag{17}$$

Proposition 5.1. *Suppose the coexistence equilibrium E_2 exists (Theorem 4.1) and $\Delta = 1 - aN^*e^{-aP^*} > 0$. If*

$$1 - \frac{2rN^*}{K}e^{-aP^*} + \frac{arN^{*2}}{K\Delta}e^{-aP^*}\left(1-e^{-aP^*}\right) > 0, \tag{18}$$

then $dD/dh < 0$, i.e., the harvesting rate h strictly decreases the Jacobian determinant D at E_2, which guarantees the transversality condition $dD/dh \neq 0$ required for the Neimark–Sacker bifurcation [20].

Proof. Since $\Delta > 0$ and $0 < e^{-aP^*} < 1$, condition (18) makes the bracketed factor in (17) strictly positive. From (16), $N_h < 0$ whenever $\Delta > 0$, since both terms in the denominator are positive. Hence $dD/dh = aN_h \times (\text{positive factor}) < 0$. □

Numerical verification. At the nominal parameter set $r = 2.4$, $K = 10$, $a = 0.35$, $h^* \approx 0.199193$ (the precise Neimark–Sacker threshold; see Appendix A), solving (2) gives $N^* \approx 4.641537$, $P^* \approx 3.039702$, so that $\Delta \approx 0.439358 > 0$ and the left-hand side of (18) evaluates to $\approx 1.162034 > 0$, confirming the hypothesis of Proposition 5.1. Substituting into (16)–(17) gives

$$N_h \approx -1.6394, \qquad P_h \approx -2.4437, \qquad \left.\frac{dD}{dh}\right|_{h^*} \approx -0.6668, \tag{19}$$

in agreement with the value reported in Section 5.4.3 and independently confirmed by central finite-difference differentiation of the equilibrium branch (relative error $< 10^{-6}$).

6 Maximum Sustainable Yield and the Harvesting–Invasion Trade-off

While the preceding sections establish when harvesting stabilizes the coexistence dynamics, a natural management question remains: *what harvesting rate maximizes the sustainable yield, and is this rate compatible with the persistence of the two-species system?* This question complements recent maximum-sustainable-yield-oriented studies of harvested discrete-time models [6, 7]. We answer it in two stages: first at the prey-only equilibrium E_1, where a closed-form solution exists; then at the coexistence equilibrium E_2, using the transversality machinery of Section 5.5.

6.1 MSY at the Predator-free Equilibrium

The sustainable yield extracted at equilibrium is $Y(h) = hN^*(h)$. At E_1, using $N_1^*(h) = K\left(1 + \dfrac{\ln(1-h)}{r}\right)$ from Section 4.2,

$$Y_1(h) = Kh + \frac{Kh}{r}\ln(1-h), \qquad h \in (0, h_{\max}), \quad h_{\max} := 1 - e^{-r}. \tag{20}$$

Proposition 6.1 (MSY at E_1)**.** *The yield function (20) satisfies $Y_1(0) = Y_1(h_{\max}) = 0$ and is strictly concave on $(0, h_{\max})$. Consequently, there exists a unique maximizer $h_{\mathrm{MSY}} \in (0, h_{\max})$, determined by the first-order condition*

$$r + \ln(1 - h_{\mathrm{MSY}}) = \frac{h_{\mathrm{MSY}}}{1 - h_{\mathrm{MSY}}}. \tag{21}$$

Proof. Differentiating (20), $Y_1'(h) = K\left[1 + \frac{1}{r}\left(\ln(1-h) - \frac{h}{1-h}\right)\right]$, whose zero is (21). Differentiating again,

$$Y_1''(h) = -\frac{K}{r}\left[\frac{1}{1-h} + \frac{1}{(1-h)^2}\right] < 0 \tag{22}$$

for all $h \in (0,1)$, so Y_1 is strictly concave. Since $Y_1(0) = Y_1(h_{\max}) = 0$ and $Y_1'(0) = K > 0$, the unique interior critical point given by (21) is the global maximum. □

Solving (21) numerically at the nominal parameter set $r = 2.4$, $K = 10$, $a = 0.35$,

$$h_{\mathrm{MSY}} \approx 0.598131, \qquad N_1^*(h_{\mathrm{MSY}}) \approx 6.201548, \qquad Y_{\max}(E_1) \approx 3.709337. \tag{23}$$

6.2 Compatibility with Predator Invasion

Recall from Section 5.2 that the predator-invasion eigenvalue is $\lambda_2 = aN_1^*(h)$, so E_1 is invasion-resistant only when $N_1^*(h) < 1/a$, i.e., $h > h_c$, where

$$h_c = 1 - \exp\left(r\left(\frac{1}{aK} - 1\right)\right). \tag{24}$$

For the nominal parameters, $h_c \approx 0.819908$ (with domain limit $h_{\max} \approx 0.909282$).

Corollary 6.2 (Naive MSY is ecologically inconsistent)**.** *Since $h_{MSY} \approx 0.5981 < h_c \approx 0.8199$, harvesting the host population at the single-species optimum h_{MSY} leaves $N_1^*(h_{\mathrm{MSY}}) \approx 6.20$, which exceeds the invasion threshold $1/a \approx 2.86$. A parasitoid population, if present, would therefore invade before the classical single-species MSY rate is reached, and the system would settle at the coexistence equilibrium E_2 rather than E_1. Consequently, the single-species MSY prescription is not self-consistent for the host–parasitoid system, and sustainable harvesting policy must instead be evaluated at E_2.*

6.3 MSY at the Coexistence Equilibrium

At E_2, the yield function $Y_2(h) = hN^*(h)$ has no closed form, since $N^*(h)$ is defined implicitly by (2). However, its critical point can be characterized using the derivative $N_h := dN^*/dh$ already obtained in Proposition 5.1 (Eq. (16)).

Proposition 6.3 (MSY at E_2)**.** *Provided E_2 exists and is a differentiable function of h on $(0, h_c)$, any interior maximizer $h_{\mathrm{MSY},2}$ of $Y_2(h)$ satisfies*

$$N^*(h_{\mathrm{MSY},2}) = -h_{\mathrm{MSY},2}\, N_h(h_{\mathrm{MSY},2}) = \frac{h_{\mathrm{MSY},2}}{(1 - h_{\mathrm{MSY},2})\left[\dfrac{r}{K} + \dfrac{a\left(1 - e^{-aP^*}\right)}{\Delta}\right]}, \tag{25}$$

with Δ as defined in Section 5.5, jointly with the equilibrium system (2).

Solving (25) together with (2) numerically (dense grid search over $h \in (0, h_c)$ followed by golden-section refinement; MATLAB code in the supplementary materials) yields

$$\begin{aligned} h_{\mathrm{MSY},2} &\approx 0.741808, & N^*(h_{\mathrm{MSY},2}) &\approx 3.252834, \\ P^*(h_{\mathrm{MSY},2}) &\approx 0.757913, & Y_{\max}(E_2) &\approx 2.412977. \end{aligned} \tag{26}$$

Table 2: Summary of MSY analysis at E_1 and E_2 ($r = 2.4$, $K = 10$, $a = 0.35$).

Equilibrium	h_{MSY}	N^* at MSY	$Y_{\max}$	Ecologically self-consistent?
E_1 (prey-only)	0.5981	6.2015	3.7093	No ($h_{\mathrm{MSY}} < h_c = 0.8199$)
E_2 (coexistence)	0.7418	3.2528	2.4130	Yes

Remark 6.4. *Notably, $h_{\mathrm{MSY},2} \approx 0.7418$ falls strictly between the Neimark–Sacker threshold $h^* \approx 0.1992$ and the invasion threshold $h_c \approx 0.8199$ – precisely the "stable node" regime illustrated in Figure 8. Thus, the two-species-consistent MSY harvesting rate not only avoids predator extinction, but also lands naturally within the locally stable (non-chaotic) parameter window, reinforcing the dual role of harvesting as both an economic and a stabilizing control lever.*

7 Numerical Simulations

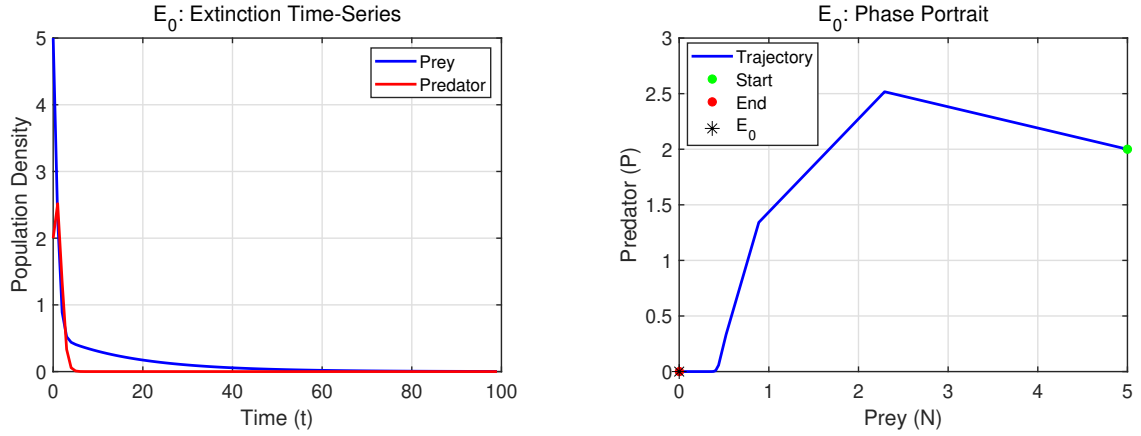
We now validate our analytical findings through numerical simulations of the following IVP using the Direct Forward Iteration Method.

7.1 Time-Series and Phase Portraits for the Three Equilibria

For each equilibrium, we present time-series and phase portraits side-by-side for the same parameter set.

7.1.1 Extinction Equilibrium E_0

Parameters: $r = 0.05, K = 10, a = 0.35, h = 0.1$.



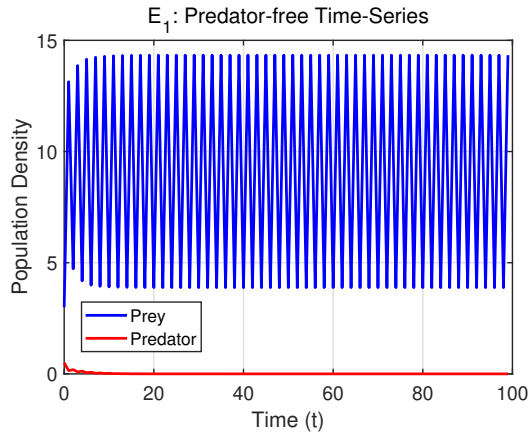
(a) Time-series

(b) Phase portrait

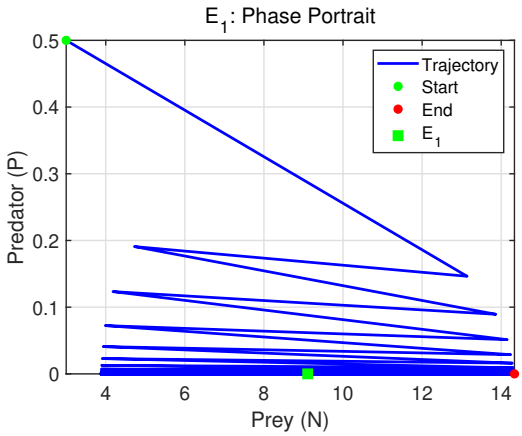
Figure 1: Extinction equilibrium $E_0(0, 0)$: (a) Time-series showing rapid decline of both populations; (b) Phase portrait with trajectory spiraling into the origin.

7.1.2 Predator-free Equilibrium E_1

Parameters: $r = 2.5, K = 10, a = 0.1, h = 0.2$.



(a) Time-series

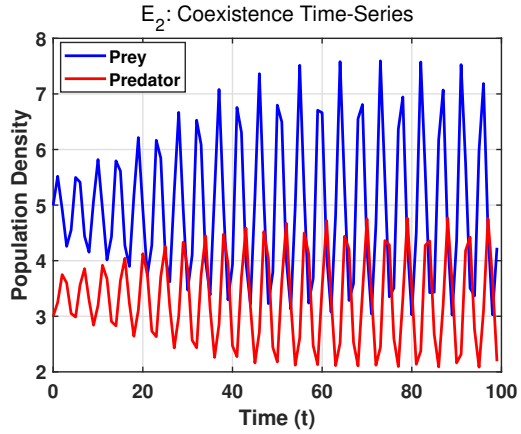


(b) Phase portrait

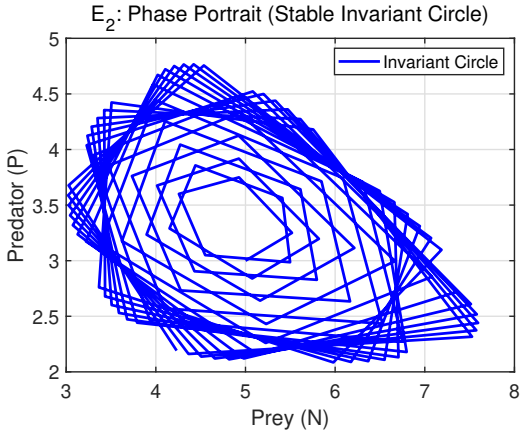
Figure 2: Prey-only equilibrium $E_1(\overline{N}, 0)$: (a) Time-series showing prey stabilization and predator extinction; (b) Phase portrait showing convergence to the prey-only fixed point.

7.1.3 Coexistence Equilibrium E_2

Parameters: $r = 2.4, K = 10, a = 0.35, h = 0.05$.



(a) Time-series

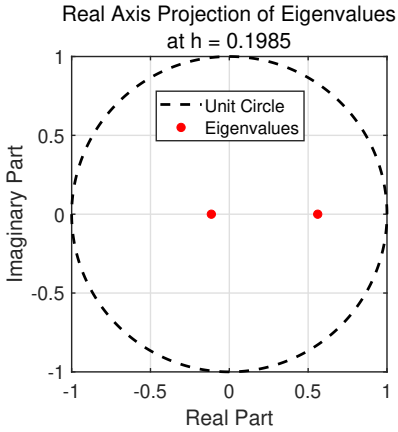


(b) Phase portrait

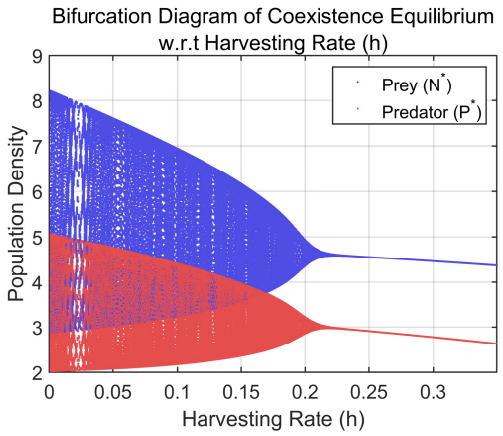
Figure 3: Coexistence equilibrium $E_2(N^*, P^*)$: (a) Time-series showing quasi-periodic oscillations; (b) Phase portrait showing a stable invariant circle.

7.2 Eigenvalue Crossing and Bifurcation

The Neimark-Sacker bifurcation occurs when the complex conjugate eigenvalues cross the unit circle.



(a) Eigenvalue crossing of the unit circle at the bifurcation threshold $h \approx 0.1985$ (rounded value used for figure generation; the analytically precise threshold is $h^* \approx 0.199193$, see Appendix A).



(b) Global bifurcation diagram showing period-doubling and chaotic bands as the harvesting rate h varies.

Figure 4: (a) Bifurcation threshold; (b) Global bifurcation diagram.

7.3 Sensitivity Analysis

The sensitivity analysis is visualized through the spectral radius and bar charts.

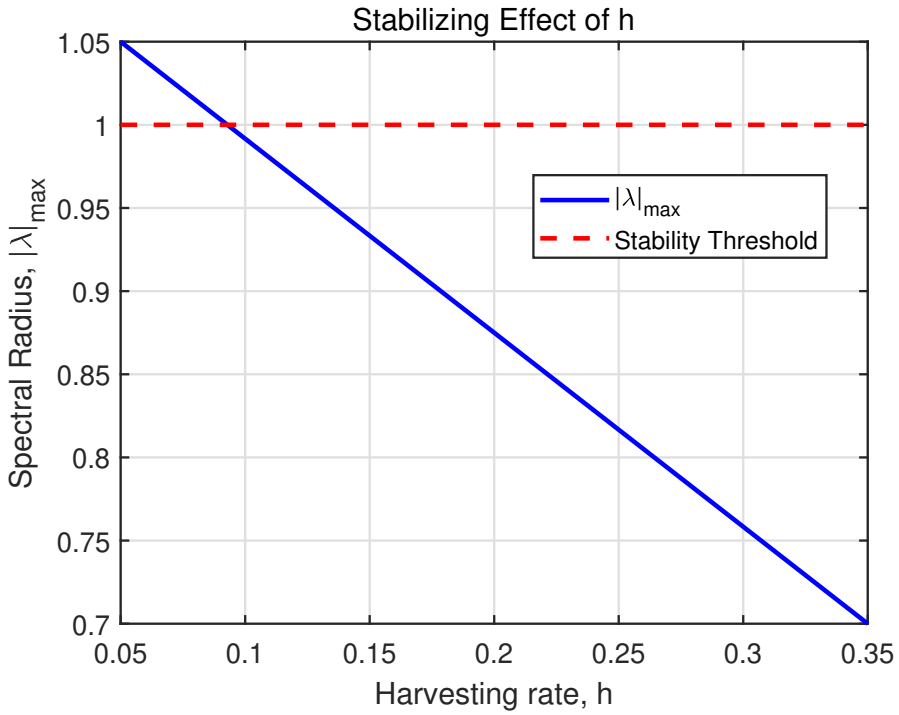


Figure 5: Spectral radius $|\lambda|_{\max}$ vs h, showing the stabilizing effect of harvesting on the interior equilibrium.

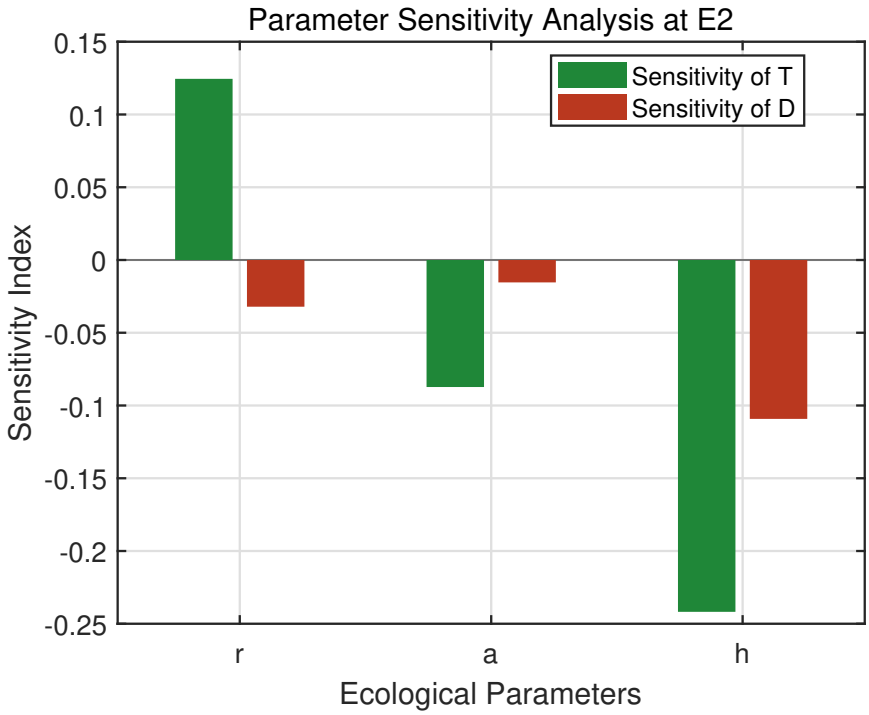


Figure 6: Normalized sensitivity indices for E_2, ranking the influence of each parameter on stability.

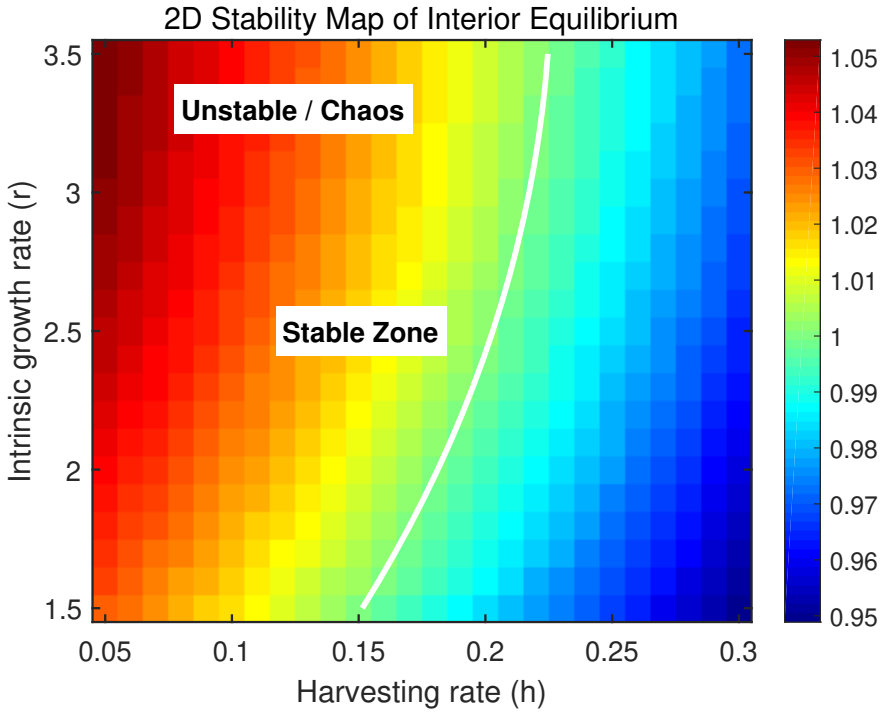


Figure 7: 2D stability map in the (h, r) parameter space. The white contour ($|\lambda| = 1$) separates the stable (dark blue) from the unstable/chaotic (yellow/red) regions.

7.4 Phase Portraits of Dynamical Regimes

The different dynamical regimes of the coexistence equilibrium are highlighted by three example phase portraits. E_2.

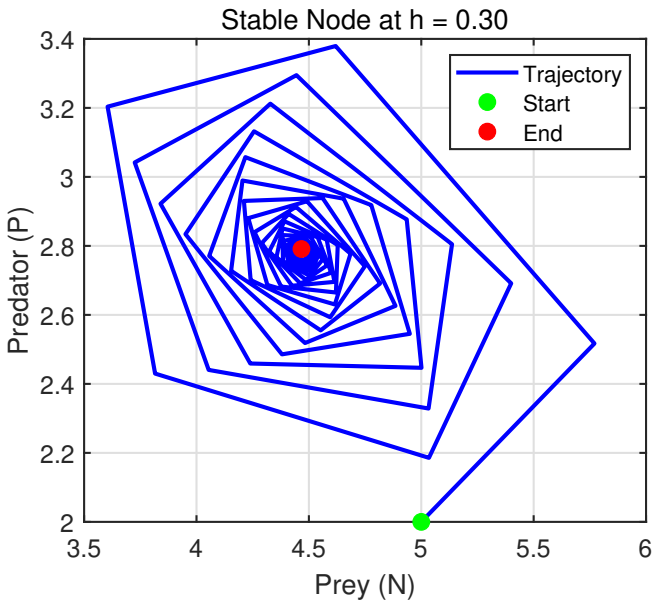
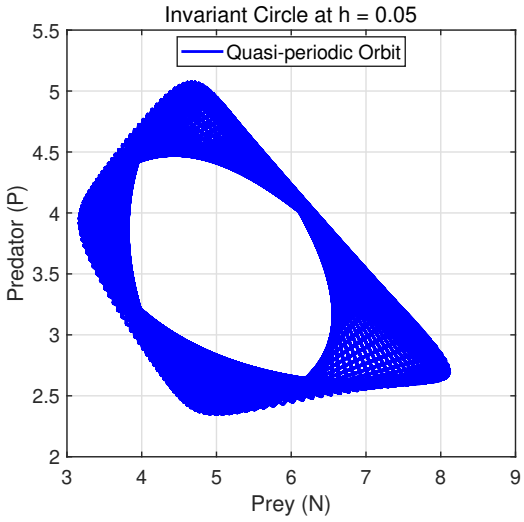
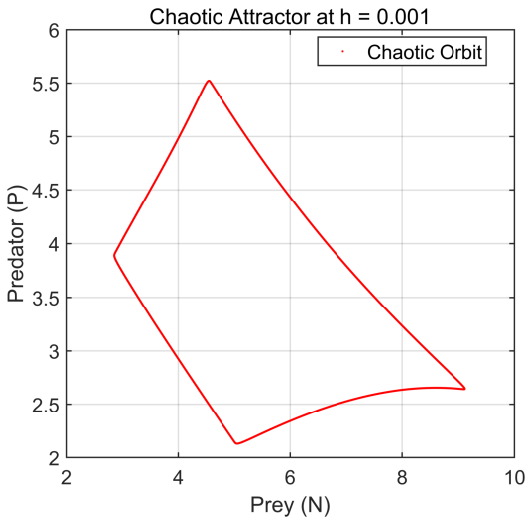


Figure 8: Stable node at $h = 0.30$. The trajectory converges directly to the interior fixed point E_2.



(a) Stable invariant circle at $h = 0.05$, indicating quasi-periodic dynamics at E_2.



(b) Chaotic attractor at $h = 0.001$, displaying fractal-like structure at E_2.

Figure 9: (a) Stable invariant circle; (b) Chaotic attractor.

8 Concluding Remarks

According to our study, proportionate harvesting has two functions: it lowers population densities and, at moderate levels, it helps stabilize the system. The harvesting rate h is the most important factor, according to the sensitivity analysis, and the 2D stability map offers precise management thresholds. Stable quasi-periodic oscillations result from the supercritical Neimark-Sacker bifurcation, but excessive harvesting reduction causes chaotic behavior. The traditional single-species harvesting optimum is therefore ecologically contradictory for this host-parasitoid system, according to the Maximum Sustainable Yield analysis (Section 6), since predator invasion would undermine it before it could be achieved. The two-species-consistent MSY rate $h_{\mathrm{MSY},2} \approx 0.742$, by contrast, is both biologically self-consistent and falls within the locally stable (non-chaotic) parameter window, offering a concrete, defensible harvesting recommendation. These findings have practical implications for fisheries management [29] and conservation biology, particularly in biological pest control contexts [27, 26] where the harvested species is the

host of a natural enemy.

We have conducted a thorough mathematical and numerical study of a discrete-time prey-predator model with proportional harvesting. Key contributions include: (i) rigorous derivation of equilibrium existence and stability, (ii) complete sensitivity analysis with a closed-form transversality proposition for the Neimark-Sacker bifurcation, (iii) analytical normal form for the Neimark-Sacker bifurcation with a fully verified first Lyapunov coefficient, (iv) a Maximum Sustainable Yield analysis revealing that single-species harvesting optima are ecologically inconsistent for host–parasitoid systems, and (v) extensive numerical validation. Our results demonstrate that proportional harvesting can act as an effective chaos-suppression tool, but careful parameter tuning – guided by the two-species-consistent MSY criterion derived here – is essential to avoid extinction. Future work will incorporate stochastic environmental fluctuations [27] and time delays, as well as refuge effects [13, 28] or fear effects [12], in the spirit of related extensions of discrete-time predator-prey frameworks.

Appendix A: Analytical Normal Form for Neimark-Sacker Bifurcation

We derive the first Lyapunov coefficient $l_1(0)$ to determine the direction of the bifurcation, following Kuznetsov [20]. Consider the map $\mathbf{x} \mapsto \mathbf{f}(\mathbf{x}, \mu)$, where $\mathbf{x} = (N - N^*, P - P^*)^T$ and $\mu = h - h^*$. The Taylor expansion up to third order is:

$$\mathbf{f}(\mathbf{x}, \mu) = J(\mu)\mathbf{x} + \frac{1}{2}B(\mathbf{x}, \mathbf{x}) + \frac{1}{6}C(\mathbf{x}, \mathbf{x}, \mathbf{x}) + O(\|\mathbf{x}\|^4),$$

where the multilinear forms are built from the Hessian and third-order partial-derivative tensors of F_1, F_2 (the two component maps of system (1)) evaluated at E_2:

$$B_i(x, y) = \sum_{j,k=1}^{2} \left.\frac{\partial^2 F_i}{\partial \xi_j \partial \xi_k}\right|_{E_2} x_j y_k, \qquad C_i(x, y, z) = \sum_{j,k,l=1}^{2} \left.\frac{\partial^3 F_i}{\partial \xi_j \partial \xi_k \partial \xi_l}\right|_{E_2} x_j y_k z_l.$$

A.1 Precise bifurcation point

Solving $D(h) = 1$ exactly (rather than using the rounded value $h = 0.1985$) gives the corrected threshold

$$h^* \approx 0.199193, \qquad N^* \approx 4.641537, \qquad P^* \approx 3.039702, \tag{27}$$

at which

$$T \approx 0.446673, \quad D = 1 \text{ (exactly)},$$
$$\lambda = e^{i\theta} \approx 0.223337 + 0.974741i, \quad \theta \approx 1.345560 \text{ rad}.$$

A.2 Jacobian at E_2

$$J(E_2) \approx \begin{pmatrix} -0.113969 & -1.624538 \\ 0.654891 & 0.560642 \end{pmatrix}. \tag{28}$$

A.3 Second- and third-order derivative tensors

The Hessian matrices of F_1 and F_2 at E_2 are

$$H_1 \approx \begin{pmatrix} -0.212647 & 0.039889 \\ 0.039889 & 0.568588 \end{pmatrix}, \qquad H_2 \approx \begin{pmatrix} 0 & 0.120788 \\ 0.120788 & -0.196225 \end{pmatrix}. \tag{29}$$

The (symmetric) third-order partial derivatives, indexed by $(j, k, l) \in \{1, 2\}^3$ with $1 \equiv N$, $2 \equiv P$, are given in Table 3.

Table 3: Third-order partial derivatives of F_1, F_2 at E_2 ($h = h^*$).

(j,k,l)	$\partial^3 F_1/\partial\xi_j\partial\xi_k\partial\xi_l$	(j,k,l)	$\partial^3 F_2/\partial\xi_j\partial\xi_k\partial\xi_l$
(N,N,N)	0.108635	(N,N,N)	0
(N,N,P)	0.074427	(N,N,P)	0
(N,P,P)	−0.013961	(N,P,P)	−0.042276
(P,P,P)	−0.199006	(P,P,P)	0.068679

A.4 Eigenvectors

The eigenvector q satisfying $Jq = \lambda q$, and the adjoint eigenvector p satisfying $J^T p = \bar{\lambda} p$ with normalization $\langle p, q\rangle := \bar{p}^T q = 1$, are

$$q \approx (-0.844213,\ 0.175285 + 0.506537\,i)^T, \tag{30}$$

$$p \approx (-0.592268 + 0.204952\,i,\ 0.987094\,i)^T. \tag{31}$$

(Verification: $\langle p, q\rangle \approx 1.0000 - 1.7 \times 10^{-18} i$.)

A.5 Multilinear form evaluations

Using H_1, H_2 (Eq. 29) and Table 3,

$$g_{20} := \langle p, B(q,q)\rangle \approx 0.050146 + 0.011746\,i, \tag{32}$$

$$g_{11} := \langle p, B(q,\bar{q})\rangle \approx 0.000000 + 0.090935\,i, \tag{33}$$

$$g_{02} := \langle p, B(\bar{q},\bar{q})\rangle \approx 0.295474 + 0.090935\,i, \tag{34}$$

$$g_{21} := \langle p, C(q,q,\bar{q})\rangle \approx 0.041815 - 0.006809\,i. \tag{35}$$

A.6 First Lyapunov coefficient

The complete Kuznetsov formula for the first Lyapunov coefficient of a Neimark–Sacker bifurcation is

$$l_1(0) = \frac{1}{2}\mathrm{Re}\big[\bar{\lambda}\, g_{21}\big] - \frac{1}{2}\mathrm{Re}\left[\frac{(1-2\lambda)\bar{\lambda}^2}{1-\lambda}\, g_{20} g_{11}\right] - \frac{1}{2}|g_{11}|^2 - \frac{1}{4}|g_{02}|^2. \tag{36}$$

Evaluating each term numerically,

$$\tfrac{1}{2}\mathrm{Re}[\bar{\lambda} g_{21}] \approx 0.001351, \tag{37}$$

$$\tfrac{1}{2}\mathrm{Re}\Big[\tfrac{(1-2\lambda)\bar{\lambda}^2}{1-\lambda} g_{20} g_{11}\Big] \approx 0.001068, \tag{38}$$

$$\tfrac{1}{2}|g_{11}|^2 \approx 0.004135, \tag{39}$$

$$\tfrac{1}{4}|g_{02}|^2 \approx 0.023894, \tag{40}$$

so that

$$l_1(0) \approx 0.001351 - 0.001068 - 0.004135 - 0.023894 \approx -0.027746 < 0. \tag{41}$$

Together with the transversality condition $dD/dh|_{h^*} \approx -0.6668 \neq 0$ (Proposition 5.1), $l_1(0) < 0$ confirms that the Neimark–Sacker bifurcation is **supercritical**, giving rise to a stable invariant circle for h slightly below h^*.

All symbolic and numerical steps above (Jacobian, Hessians, third-order tensor, eigenvector computation, and the final coefficient) were independently verified using both a Python/SymPy pipeline and a MATLAB R2018a Symbolic Math Toolbox script, with results agreeing to within 10^{-6}.

References

[1] R. M. May. Simple mathematical models with very complicated dynamics. *Nature*, 261:459–467, 1976. https://doi.org/10.1038/261459a0.

[2] S. N. Elaydi. *Discrete Chaos: With Applications in Science and Engineering*. Chapman & Hall/CRC, 2nd edition, 2008.

[3] Y. Ji, L. Lai, S. Zhong, and L. Zhang. Bifurcation and chaos of a new discrete fractional-order logistic map. *Communications in Nonlinear Science and Numerical Simulation*, 57:352–358, 2018. https://doi.org/10.1016/j.cnsns.2017.10.009.

[4] M. G. Neubert. A simple population model with qualitatively uncertain dynamics. *Journal of Theoretical Biology*, 189:399–411, 1997. https://doi.org/10.1006/jtbi.1997.0258.

[5] S. J. Schreiber. Allee effects, extinctions, and chaotic transients in simple population models. *Theoretical Population Biology*, 64:201–209, 2003. https://doi.org/10.1016/S0040-5809(03)00072-8.

[6] M. Ruan, X. Li, Y. Yu, and F. Qian. Transcritical bifurcation and Neimark-Sacker bifurcation in a discrete predator-prey model with constant-effort harvesting. *Mathematics*, 13:3935, 2025. https://doi.org/10.3390/math13243935.

[7] A. Suryanto, I. Darti, and E. Cahyono. Bifurcation analysis and chaos control of a discrete-time fractional order predator-prey model with Holling type II functional response and harvesting. *Chaos Theory and Applications*, 7(1):87–98, 2025. https://doi.org/10.51537/chaos.1581247.

[8] J. D. Murray. Mathematical Biology I: An Introduction. Interdisciplinary Applied Mathematics, Vol. 17, Springer-Verlag, New York, 3rd edition, 2002.

[9] J. R. Beddington, C. A. Free, and J. H. Lawton. Dynamic complexity in predator-prey models framed in difference equations. Nature, 255:58–60, 1975. https://doi.org/10.1038/255058a0.

[10] Q. Din. Global stability of Beddington model. *Qualitative Theory of Dynamical Systems*, 2016. https://doi.org/10.1007/s12346-016-0197-9.

[11] A. Q. Khan, I. M. Alsulami, and S. K. A. Hamdani. Controlling the chaos and bifurcations of a discrete prey-predator model. *AIMS Mathematics*, 9(1):1783–1818, 2024. https://doi.org/10.3934/math.2024087.

[12] C. Lei, X. Han, and W. Wang. Bifurcation analysis and chaos control of a discrete-time prey-predator model with fear factor. *Mathematical Biosciences and Engineering*, 19(7):6659–6679, 2022. https://doi.org/10.3934/mbe.2022313.

[13] P. A. Naik, M. Amer, R. Ahmed, S. Qureshi, and Z. Huang. Stability and bifurcation analysis of a discrete predator-prey system of Ricker type with refuge effect. *Mathematical Biosciences and Engineering*, 21(3):4554–4586, 2024. https://doi.org/10.3934/mbe.2024201.

[14] W. Liu and D. Cai. Bifurcation, chaos analysis and control in a discrete-time predator-prey system. *Advances in Difference Equations*, 2019:11, 2019. https://doi.org/10.1186/s13662-019-1950-6.

[15] A. Singh and P. Deolia. Dynamical analysis and chaos control in discrete-time prey-predator model. *Communications in Nonlinear Science and Numerical Simulation*, 90:105313, 2020. https://doi.org/10.1016/j.cnsns.2020.105313.

[16] Işık, Seval and Kangalgil. On the analysis of stability, bifurcation, and chaos control of discrete-time predator-prey model with Allee effect on predator. *Hacettepe Journal of Mathematics and Statistics*, 51(2):404–420, 2022. https://doi.org/10.15672/hujms.728889.

[17] A. Q. Khan. Neimark-Sacker bifurcation of a two-dimensional discrete-time predator-prey model. *SpringerPlus*, 5:126, 2016. https://doi.org/10.1186/s40064-015-1618-y.

[18] B. Hong and C. Zhang. Neimark-Sacker bifurcation of a discrete-time predator-prey model with prey refuge effect. *Mathematics*, 11:1399, 2023. https://doi.org/10.3390/math11061399.

[19] U. Saeed, I. Ali, and Q. Din. Neimark-Sacker bifurcation and chaos control in discrete-time predator-prey model with parasites. *Nonlinear Dynamics*, 94:2527–2536, 2018. https://doi.org/10.1007/s11071-018-4507-4.

[20] Y. A. Kuznetsov. *Elements of Applied Bifurcation Theory*. Springer-Verlag, New York, 3rd edition, 2004.

[21] X. Ma, Q. Din, M. Rafaqat, N. Javaid, and Y. Feng. A density-dependent host-parasitoid model with stability, bifurcation and chaos control. *Mathematics*, 8(4):536, 2020. https://doi.org/10.3390/math8040536.

[22] A. Q. Khan and M. N. Qureshi. Dynamics of a modified Nicholson-Bailey host-parasitoid model. *Advances in Difference Equations*, 2015:23, 2015. https://doi.org/10.1186/s13662-015-0357-2.

[23] Q. Din, Ö. A. Gümüş, and H. Khalil. Neimark-Sacker bifurcation and chaotic behaviour of a modified host-parasitoid model. *Zeitschrift für Naturforschung A*, 72(1):25–37, 2017. https://doi.org/10.1515/zna-2016-0335.

[24] K. Marcinko and M. Kot. A comparative analysis of host-parasitoid models with density dependence preceding parasitism. *Journal of Biological Dynamics*, 14:479–514, 2020 https://doi.org/10.1080/17513758.2020.1783005.

[25] S. R. J. Jang and J. L. Yu. Discrete-time host–parasitoid models with pest control. *Journal of Biological Dynamics*, 6(2):718–739, 2012. https://doi.org/10.1080/17513758.2012.700074.

[26] Q. Din and U. Saeed. Bifurcation analysis and chaos control in a host-parasitoid model. *Mathematical Methods in the Applied Sciences*, 40(11):4395, 2017. https://doi.org/10.1002/mma.4395.

[27] A. Singh. Stochasticity in host-parasitoid models informs mechanisms regulating population dynamics. *Scientific Reports*, 11:16749, 2021. https://doi.org/10.1038/s41598-021-96212-y.

[28] Q. Din, W. Ishaque, M. A. Iqbal, and U. Saeed. Modification of Nicholson-Bailey model under refuge effects with stability, bifurcation, and chaos control. *Journal of Vibration and Control*, 28(23-24):3524–3538, 2021/2022. https://doi.org/10.1177/10775463211034021.

[29] W. E. Ricker. Stock and recruitment. *Journal of the Fisheries Research Board of Canada*, 11(5):559–623, 1954. https://doi.org/10.1139/f54-039.

[30] M. Monzu Uddin, M. Sakib, and M. Kabir. BioPest: An integrated deep learning driven predator–prey framework for early pest detection and biological control. *Engineering Reports*, 8, 2026. https://doi.org/10.1002/eng2.70943.

[31] M. S. Akber, M. M. Hasan, M. H. Kabir, and M. O. Gani. Population projection of Southeast Asia with a time-delay logistic model. *Bulletin of Biomathematics*, 3(1):1–20, 2025. https://doi.org/10.59292/bulletinbiomath.1707070.